Proceedings World Geothermal Congress 2026
Calgary, Canada, June 8 – 11, 2026

Advancing Geothermal Reservoir Characterization through Process-Based Fracture Forward Modelling: A Case Study from the Cretaceous Formation in the Eclépens Region of the Swiss Molasse Basin.

Salmon Lucy[1]*, Deb Paromita[1] and Welch Michael[2]
[1]Swiss Geo Energy, Geneva, Switzerland, [2]Technical University of Denmark, Kongens Lyngby, Denmark
*lucy.salmon@swissgeoenergy.com

Keywords: Process-based Fracture Forward Modelling, Swiss Molasse Basin, Muschelkalk Formation, Geothermal exploration, Fracture propagation

INTRODUCTION & OBJECTIVES

Carbonate sedimentary rocks hold significant potential for groundwater storage and geothermal energy, yet their effectiveness relies strongly on the presence and connectivity of faults and fractures (Guerriero et al., 2015; Welch et al., 2019). Accurate characterization of fracture parameters is therefore essential for reducing exploration uncertainty and de-risking geothermal projects. Traditional fracture modelling methods use geostatistics to extrapolate reservoir properties in data poor areas (e.g. Amanbek et al., 2023; Andersson et al., 1984, Chandna et al., 2019; Gao et al., 2025; Srivastava et al., 2004). While useful, they lose reliability with increasing distance from control points leading to high exploration risks. In contrast, process-based forward fracture modelling (FFM) simulates geological evolution and mechanical deformation based on the known response of the system to defined boundary and input conditions (Cross and Lessenger, 1999; Watney et al., 1999), improving the physical consistency and predictive robustness of reservoir characterization (Lessenger, 1993). In this context, the GO-Forward project (Geothermal Exploration and Optimization through Forward Modelling and Resource Development), a four-year (2024-2028) European initiative, aims to develop process-based fracture forward modelling approach that simulates fracture nucleation and propagation by modelling the impact of the major deformation events utilizing empirical geomechanical principles (Welch, 2023). While such formulations are well established (Olson, 2004; Davy et al., 2013), GO-Forward applies the novel Petrel DFM Generator plug-in (Welch et al., 2019), which combines fracture scaling laws, subcritical propagation theory, and linear elastic fracture mechanics (LEFM) to create realistic 3D fracture networks. Such models require independent field datasets for input, calibration, and validation. In this work, we test the FFM code in the Eclépens region of the Swiss Molasse Basin, a structurally complex area with high geothermal potential (Scheidt Schmitt, 2020) serving as a key test site for model development. The DFM Generator is used to simulate the fracture network in the Lower Cretaceous unit, where sufficient subsurface and outcrop information is available to calibrate and validate the model's performance. Once validated, the FFM code will be applied to other fracture dominated units with limited subsurface data but promising geothermal prospects.

1 GEOLOGICAL CONTEXT

The study region lies in the Swiss Molasse Basin (SMB), a foreland basin formed during the Alpine orogeny and composed of mildly deformed Mesozoic–Cenozoic sediments overlying the crystalline basement (Sommaruga et al., 2012 and references therein). The target area sits between the two branches of the La Sarraz–Mormont Fault System (SMFS), a dextral strike-slip fault zone at the transition between the Jura Fold-and-Thrust Belt and the Plateau Molasse. This region is marked by stress heterogeneity and structural anisotropy (Scheidt Schmitt, 2020) (Figure 1.1). Deformation of the SMB began no earlier than ~40 Ma and older indicators were largely overprinted by the Alpine orogeny (Burkhard & Sommaruga, 1998). Two Cenozoic tectonic phases are documented. The Paleogene extensional phase comprises late Eocene NNE–SSW strike-slip and Oligocene NW–SE extension. These regimes predate Molasse deposition and are therefore not recorded in the Molasse (Ibele, 2011; Radaideh and Mosar, 2021). The Neogene compressive phase includes Miocene NW–SE compression, which reactivated Mesozoic structures, and Late Miocene to present NNW–SSE strike-slip, which affected the previously unstructured Molasse cover. In this work, we focus on modelling the impact of the recent strike-slip regime.

The well-documented Lower Cretaceous Urgonian unit provides the basis for model calibration and validation. It consists mainly of shallow-marine fractured carbonates, including oolitic grainstones, micritic limestones, and marls (Figure 1.1). Outcrop, core, and well data reveal intense fracturing in the Upper Urgonian, particularly near faults (Doesburg, 2023; Scheidt Schmitt, 2020).

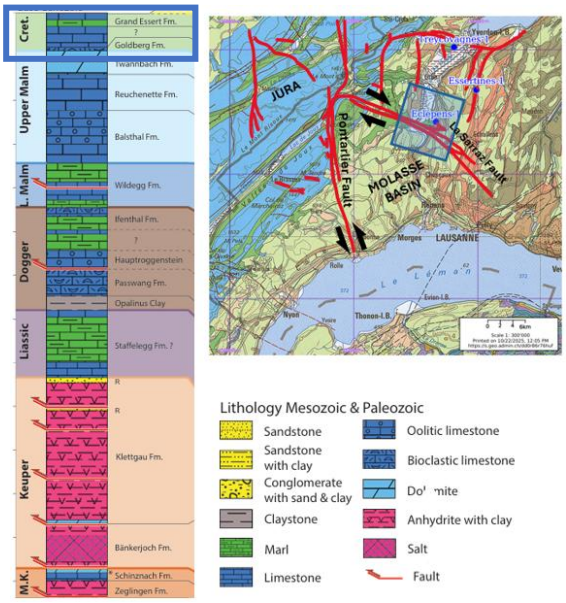

Figure 1.1. Left: Stratigraphic column of the study area from the Treycovagnes-1 well (Gruber, 2017). The blue square indicates the interval of interest. Upper right: Geological map of Western Switzerland showing the study area (blue square), main regional faults (red lines) and constraining wells (blue dots) (modified from Swisstopo).

2 METHODS

2.1 Characterization of fractured intervals

We defined the main fractured intervals within the Lower Cretaceous succession based on dipmeter measurements from the Eclépens-1 well. We identified zones of higher fracture density between 202 and 242 m MD, which were selected as modelling targets (Figure 2.1). To account for the presence of marl interbeds, interpreted as barriers to fracture propagation, we adjusted the layer thicknesses of the structural grid to reflect only the carbonate intervals. We projected the well trajectory and dipmeter data onto the structural grid to locate precisely the fractured layers, which were then selected for the forward modelling workflow.

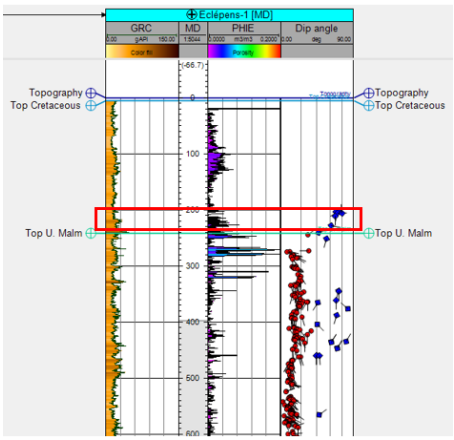

Figure 2.1. Modelled interval within the Lower Cretaceous (red square). The left column shows the gamma-ray log, the middle column the effective porosity, and the right column the dipmeter data with dip classifications: fractures are shown in blue and bedding planes in red.

2.2 Fracture drivers

Fracturing is driven by a combination of regional tectonic strain, and local stress induced by displacement on major faults. These loads are applied at a constant rate until the fracture network becomes saturated. Assuming a purely elastic, uncompacted layer, we estimated the regional in-situ principal stresses from 3D Hooke's Law using externally applied horizontal strains as boundary conditions. The effective vertical stress was computed as the difference between lithostatic and pore fluid pressure. Taking the vertical stress as a principal component, the horizontal stresses were obtained from the isotropic elastic constitutive relationship expressed

through Young's modulus and Poisson's ratio (Welch et al., 2020). We iteratively adjusted the initial strains to ensure that (1) the minimum horizontal strain is less than the maximum; (2) the principal stresses are consistent with the expected hierarchy for strike-slip Andersonian regime; (3) the resulting stress ratio lies within the range reported by Radaideh and Mosar (2021) and (4) all principal stresses are compressive (conventionally considered positive). The resulting stress magnitudes served as input for the tectonic modelling, which models the local stress variations around the major faults. Using these results, the azimuth of minimum horizontal strain and the magnitudes of the minimum and maximum horizontal strain rates across the study area were determined using tensor algebra and eigenvalue decomposition (Allmendinger et al., 2012; Newman, 2012). The strain maps make it possible to account for the influence of faults without explicitly modeling them in the grid, thereby reducing geometrical artefacts.

2.3 Elastic rock properties and depth of burial

We assumed that fracturing occurred close to present burial depth, and that therefore the elastic rock properties then were similar to current values. We estimated them using empirical correlations derived from wireline logs. Young's modulus and Poisson's ratio estimates were unavailable for the Lower Cretaceous, but since the fractured interval lies near the Top Upper Malm, and the Upper Malm and Lower Cretaceous show similar effective porosity (2.1% VS 1.4% respectively) and gamma ray responses (20 gAPI VS 24 gAPI respectively), we used measured values from the underlying Upper Malm formation for the modelling process. Accordingly, we defined Young's modulus = 25.75 GPa and Poisson's ratio = 0.26. The top of the fractured interval lies at ~200 m depth but is not mapped on seismic data. Since it is closer to the mapped Top Upper Malm than the mapped Top Lower Cretaceous horizon, we defined a synthetic depth surface constrained to the Upper Malm geometry and placed 40 m above the Upper Malm horizon. This accurately represents the fractured interval thickness and enables an improved prediction of overburden pressure and vertical effective stress that plays a key role in formation and nucleation of fracture network.

2.4 Calibration dataset

The calibration dataset combines outcrop data from the Eclépens and Bui quarries with borehole observations from Eclépens-1, GEo-01, and GEo-02. In the Lower Cretaceous Urgonian limestones, fractures are subvertical (dipping 60–80°) and predominantly strike NW–SE and NE–SW, with subordinate N–S orientations consistent with the regional stress field (Figure 2.2). Local variability occurs near fault zones, where multiple conjugate sets develop (Scheidt Schmitt, 2020). Fracture intensity varies with depth, reaching up to 1 fracture/m in the Chambotte and 0.67 fractures/m in the Grand Essert formations (Doesburg, 2023). A tentative structural linkage between these fracture patterns and Thin Fault Likelihood (TFL) predictions was used to predict spatial and directional trends from seismic attributes though this approach remains experimental.

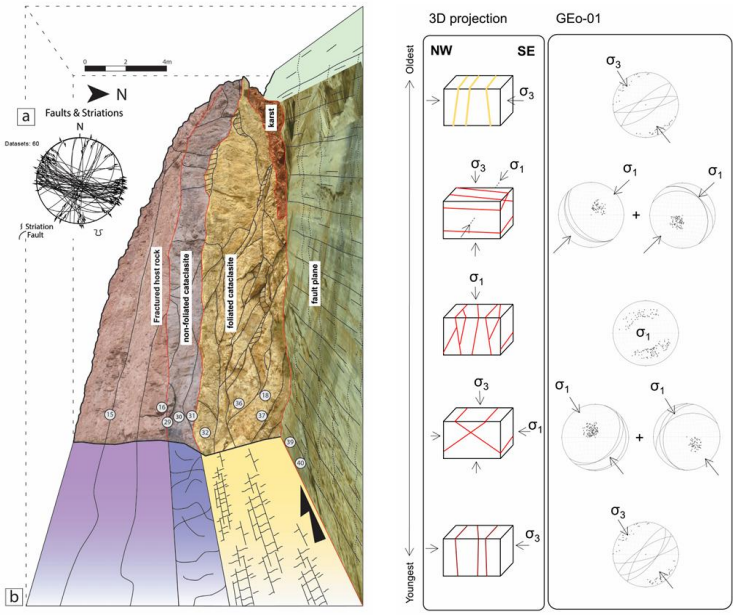

Figure 2.2. Left: a) Stereonet of 60 fault-plane orientations (azimuth and dip) and striations from the Mormont Fault at the Eclépens Holcim quarry. b) Vertical fault plane. Circles show sampling positions (Scheidt Schmitt, 2020). Right: Interpretation of the GEo-01 fractures in terms of sets and associated stress regimes (Doesburg, 2023).

3 PRELIMINARY RESULTS AND DISCUSSION

Figure 3.1 A) shows the modeled fracture network in the Base Lower Cretaceous layer for the strike-slip deformation event lasting from the Miocene to the present day. The model shows the growth and propagation of fractures after 4.14 Ma of tectonic evolution. Darker areas in the northwest in Figure 3.1A indicate higher fracture density. The fractures initiate in the northwest and propagate toward the southeast. This pattern is most likely controlled by the depth of the formation. As the geological layers are deeper in the south-eastern part of the study area, they have higher confining stress. As such, the fractures require greater strain accumulation to initiate in this area. The lack of fractures in the vicinity of the faults (blank areas next to faults shown in blue in Figure 3.1A reflects the influence of stress shadows around them. Early fractures nucleate and propagate in the direction NNW–SSE (dark blue arrows) and WNW-ESE (orange arrows) in conjugate sets (Figure 3.1C). As deformation progresses, secondary, shorter NNE-SSW striking fractures (purple arrows) develop between major traces, producing an anisotropic mosaic network. Near the faults, the fractures develop slightly curved geometries due to local stress perturbations. All fractures are subvertical or steeply inclined. The pattern is consistent with the regional NE–SW extension (light blue arrows), field observations, and the fault orientations observed in the Thin Fault Likelihood (TFL) predictions shown in Figure 3.1D.

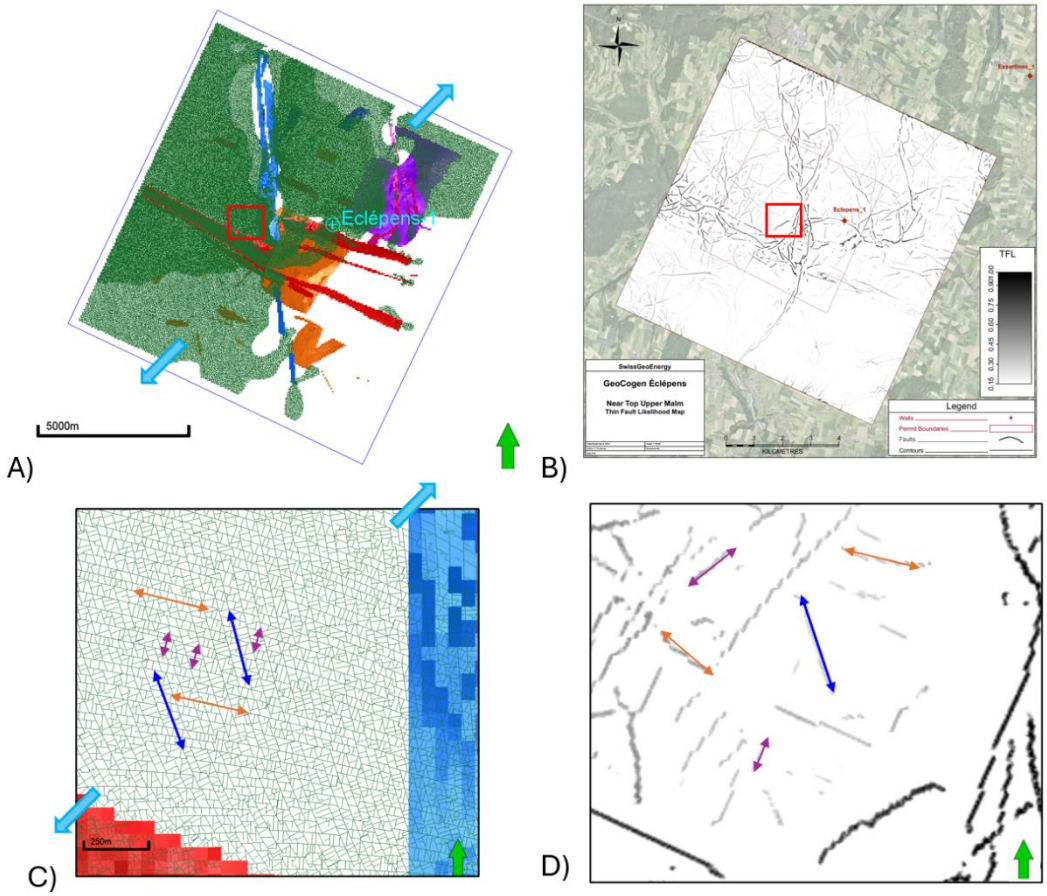

Figure 3.1. A) Modelled fracture network for the strike-slip deformation event lasting from the Miocene to–present regime in the Lower Cretaceous formation. Light blue arrows show the direction of minimum stress. B) Thin Fault Likelihood (TFL) seismic attribute extracted close to the Lower Cretaceous formation. The red rectangle shows the outline of the area enlarged in figures C and D. C and D) Close-ups of the modelled fracture network and the TFL seismic attribute, respectively, showing agreement in the main fracture orientations NNW–SSE (dark blue), WNW–ESE (orange), and NNE–SSW (purple).

4 CONCLUSIONS AND WAY FORWARD

Overall, the preliminary modeling results show good agreement with regional field observations, especially the orientations and the fracture clustering near faults as shown in Figure 3.1C andD. Further work will focus on sensitivity analyses to evaluate the impact of key inputs such as elastic properties, flexural strains, fluid pressure gradient, and fracture propagation rate on the geometry, distribution, and fracture network properties. The scope of work will also be extended to other stratigraphic formations and major tectonic events. The results will be further validated by comparing them with the fracture properties obtained from borehole images and outcrop

analogues for the stratigraphic formations where we have sufficient data. Once validated, the workflow will be applied to data-poor fractured units with high geothermal potential to assess its value for geothermal characterization.

Acknowledgements

The European part of this project is funded by the European Union under the Horizon Europe programme (grant no. 101147618). Views and opinions expressed are those of the authors only and do not necessarily reflect those of the European Union or CINEA. Neither the European Union nor CINEA is responsible for them. The Swiss part is funded by the Swiss Confederation, Federal Department of Economic Affairs, Education and Research (EAER), State Secretariat for Education, Research and Innovation (SERI).

REFERENCES

Allmendinger, R.W., Cardozo, N., and Fisher, D.M.: Structural Geology Algorithms, Vectors and Tensors, Cambridge University Press, (2012).

Amanbek, Y., Merembayev, T., and Srinivasan, S.: Framework of fracture network modeling using conditioned data with sequential Gaussian simulation, Arab J Geosci, 16, (2023), 219. https://doi.org/10.1007/s12517-022-11073-7

Andersson, J.: A stochastic model of a fractured rock conditioned by measured information, Water Resources Research, 20(1), (1984), 79–88.

Burkhard, M., and Sommaruga, A.: Evolution of the western Swiss Molasse Basin: Structural relations with the Alps and the Jura belt, in: Mascle, A., Puigdefábregas, C., Luterbacher, H.P., and Fernández, M. (eds), Cenozoic Foreland Basins of Western Europe, Geological Society Special Publication 134, London, (1998), 279–298. https://doi.org/10.1144/GSL.SP.1998.134.01.13

Chandna, A., and Srinivasan, S.: Modeling natural fracture networks using improved geostatistical inferences, Energy Procedia, 158, (2019), 6073–6078. https://doi.org/10.1016/j.egypro.2019.01.508

Cross, T.A., and Lessenger, M.A.: Construction and application of a stratigraphic inverse model, in: Harbaugh, J.W., Watney, W.L., Rankey, E.C., Slingerland, R., Goldstein, R.H., and Franseen, E.K. (eds), Numerical Experiments in Stratigraphy: Recent Advances in Stratigraphic and Sedimentologic Computer Simulations, SEPM Special Publication 62, SEPM Society for Sedimentary Geology, Tulsa, (1999). https://doi.org/10.2110/pec.99.62.0069

Davy, P., Le Goc, R., and Darcel, C.: A model of fracture nucleation, growth and arrest, and consequences for fracture density and scaling, Journal of Geophysical Research: Solid Earth, 118, (2013), 1393–1407. https://doi.org/10.1002/jgrb.50120

Doesburg, R.: Uncertainty reduction in image-log fracture interpretation: A study of Upper Cretaceous limestones in the Greater Geneva Basin, Switzerland, Master's thesis, Delft University of Technology, Delft, (2023). https://repository.tudelft.nl/record/uuid:a16d4d2b-d373-48a7-9e5c-b6f22d3045d0

Gao, D., Ma, L., Qian, J., et al.: Stochastic modeling of discrete fracture network considering spatial pattern and variability of fracture distribution, Geosciences Journal, 29, (2025), 290–306. https://doi.org/10.1007/s12303-025-00019-2

Guerriero, V., Dati, F., Giorgioni, M., Iannace, A., Mazzoli, S., and Vitale, S.: The role of stratabound fractures for fluid migration pathways and storage in well-bedded carbonates, Italian Journal of Geosciences, 134(3), (2015), 383–395. https://doi.org/10.3301/ijg.2014.27

Ibele, T.: Tectonics of the Western Swiss Molasse Basin during Cenozoic times, Doctoral dissertation, Université de Fribourg, Switzerland, (2011). https://sonar.ch/global/documents/302287

Lessenger, M.A.: Forward and inverse simulation models of stratal architecture and facies distributions in marine shelf to coastal plain environments, Ph.D. thesis, Colorado School of Mines, Golden, (1993). https://repository.mines.edu/handle/11124/177235

Newman, W.I.: Continuum Mechanics in the Earth Sciences, Cambridge University Press, (2012).

Olson, J.E.: Predicting fracture swarms – the influence of subcritical crack growth and the crack-tip process zone on joint spacing in rock, in: Cosgrove, J.W., and Engelder, T. (eds), The Initiation, Propagation, and Arrest of Joints and Other Fractures, Geological Society Special Publications, 231, London, (2004), 73–87. https://doi.org/10.1144/GSL.SP.2004.231.01.05

Radaideh, O.M.A., and Mosar, J.: Cenozoic tectonic deformation along the Pontarlier strike-slip fault zone (Swiss and French Jura fold-and-thrust belt): Insights from paleostress and geomorphic analyses, Tectonics, 40, (2021), e2021TC006758. https://doi.org/10.1029/2021TC006758

Scheidt Schmitt, N.C.: Fault anatomy, porosity and pore connectivity: The La Sarraz-Mormont Fault System, Doctoral dissertation, Université de Fribourg, Switzerland, Thesis No. 2176, (2020).

Sommaruga, A., Eichenberger, U., and Marillier, F.: Seismic Atlas of the Swiss Molasse Basin, Matériaux Géol. Suisse, Géophys., 44, Swiss Geophysical Commission, (2012).

Srivastava, R.M., Frykman, P., and Jensen, M.: Geostatistical simulation of fracture networks, in: Leuangthong, O., and Deutsch, C.V. (eds), Geostatistics Banff 2004, Quantitative Geology and Geostatistics, 14, Springer, Dordrecht, (2005). https://doi.org/10.1007/978-1-4020-3610-1_30

Watney, W.L., Rankey, E.C., and Harbaugh, J.: Perspectives on stratigraphic simulation models: Current approaches and future opportunities, in: Harbaugh, J.W., Watney, W.L., Rankey, E.C., Slingerland, R., Goldstein, R.H., and Franseen, E.K. (eds), Numerical Experiments in Stratigraphy: Recent Advances in Stratigraphic and Sedimentologic Computer Simulations, SEPM Special Publication 62, SEPM Society for Sedimentary Geology, Tulsa, (1999). https://doi.org/10.2110/pec.99.62.0003

Welch, M.J.: Using geomechanical models to simulate the growth of the fracture network in the Ekofisk Formation of the Kraka Structure, Danish Central Graben, in: Welch, M.J., and Lüthje, M. (eds), Geomechanical Controls on Fracture Development in Chalk and Marl in the Danish North Sea, Springer, Switzerland, (2023), 167–200. https://doi.org/10.1007/978-3-031-35327-7_7

Welch, M.J., Luthje, M., and Glad, A.C.: Influence of fracture nucleation and propagation rates on fracture geometry: Insights from geomechanical modelling, Petroleum Geoscience, 25(4), (2019), 473–485. https://doi.org/10.1144/petgeo2018-161

Welch, M.J., Lüthje, M., and Oldfield, S.J.: Modelling the Evolution of Natural Fracture Networks: Methods for Simulating the Nucleation, Propagation and Interaction of Layer-Bound Fractures, Springer, Cham, (2020), 230 pp. https://doi.org/10.1007/978-3-030-52414-2

Witter, J.B., Trainor-Guitton, W.J., and Siler, D.L.: Uncertainty and risk evaluation during the exploration stage of geothermal development: A review, Geothermics, 78, (2019), 233–242. https://doi.org/10.1016/j.geothermics.2018.12.011